Int. J. Environ. Sci. Technol. (2015) 12:1283–1294
DOI 10.1007/s13762-014-0507-1

ORIGINAL PAPER

Arsenic(III) removal from aqueous solution by raw and zinc-loaded pine cone biochar: equilibrium, kinetics, and thermodynamics studies

N. Van Vinh · M. Zafar · S. K. Behera · H.-S. Park

Received: 31 July 2013 / Revised: 12 December 2013 / Accepted: 11 January 2014 / Published online: 29 January 2014

Abstract The potential of raw pine cone (PC) biochar and its modified form (Zn-loaded biochar) was evaluated for the removal of trivalent arsenic [As(III)] from the aqueous solution. The influence of treatment of PC biochar with $Zn(NO_3)_2$ on the physico-chemical properties of biochar was examined using elemental analyzer, surface area analyzer, thermo-gravimetric analyzer, Fourier transform infrared spectroscopy, and scanning electron microscopy. Experimental results revealed that the removal of As(III) was almost consistent (66.08 ± 3.94 and 87.62 ± 3.88 % on raw and Zn-loaded biochar, respectively) over an acidic pH range of 2–4 as a consequence of high affinity between the positively charged biochar surface and the predominant arsenic species (H_3AsO_3 and $H_2AsO_4^-$), followed by a decrease with increase in pH in the range of 4–12. Langmuir isotherm model was well fitted to the experimental equilibrium data ($R^2 = 0.93$) rendering the maximum adsorption capacity of 5.7 and 7.0 μg g^{-1} on raw and Zn-loaded PC biochar, respectively. The adsorption of As(III) was well represented by pseudo-second order with reaction rate constant (k_2) of 0.040 and 0.282 mg g^{-1} min on raw and zinc-loaded PC biochar, respectively, and was mainly controlled by boundary layer diffusion followed by some extent of intra-particle diffusion. The adsorption process was spontaneous with Gibb's free energy ($\Delta G°$, −4.42 ± 0.72 and −11.86 ± 1.78 kJ mol^{-1}) and exothermic in nature with enthalpy ($\Delta H°$, 13.25 and 31.10 kJ mol^{-1}) and entropy ($\Delta S°$, 0.058 and 0.141 kJ mol^{-1} K^{-1}) for raw and zinc-loaded adsorbent, respectively.

Keywords Pine cone · Biochar · Arsenic removal · Equilibrium · Kinetics · Thermodynamic

Introduction

Groundwater contamination by heavy metals has been recognized as a global environmental threat that has emanated largely due to the increase in effluent discharge from the mining and electroplating industries. These effluents contain high levels of cadmium, mercury, copper, arsenic, and lead among which arsenic (As) has been considered as the most toxic heavy metal to aquatic flora and fauna even in very low concentrations (Mohan et al. 2007). In the aquatic environment, it exists in different forms such as arsenious (H_3AsO_3, H_3AsO_3, $H_3AsO_3^{2-}$), arsenic (H_3AsO_4, H_3AsO^{4-}, $H_3AsO_4^{2-}$), arsenites [As(III)], arsenates [As(V)], methylarsenic, dimethylarsinic acid, and arsine (Mohan and Pittman 2007). Its long-term exposure causes a variety of serious health issues such as dermal changes (pigmentation, hyperkeratoses, and ulceration), respiratory, neurological, cardiovascular, vomiting as well as results in the appearance of diverse type of cancer of skin, lung, bladder, and kidney (Guo et al. 2007; Mandal and Suzuki 2002; Kamsonlian et al. 2012). The toxicity of As exists greatly in its oxidation states (−3, 0, +3, and +5), and the trivalent form [As(III)] is recognized as most hazardous state (Manju et al. 1998). The World Health

N. Van Vinh · H.-S. Park (✉)
Department of Civil and Environmental Engineering, University of Ulsan, Ulsan, Republic of Korea
e-mail: parkhs@ulsan.ac.kr

M. Zafar · S. K. Behera · H.-S. Park
Center for Clean Technology and Resource Recycling, University of Ulsan, Ulsan, Republic of Korea

S. K. Behera
Chemical Engineering Department, GMR Institute of Technology, Rajam, Srikakulam Dist 532127, AP, India

Organization (WHO), the European Union (EU), and several countries including Japan, India, China, Bangladesh, and Vietnam have recommended its maximum contaminant level (MCL) of 10 μg L^{-1} in drinking water (Mohan and Pittman 2007; Urík et al. 2009; Mafu et al. 2013).

There are many technologies, viz. enhanced coagulation, membrane systems, ion exchange, adsorption, lime softening, and oxidation processes being available for the removal of arsenic from wastewater/drinking water (Ghanizadeh et al. 2010; Akter and Ali 2011). Among them, adsorption process is cost-effective, flexible, and easy to design and operate. Several types of absorbent including iron-containing granular activated carbon (GAC) (Gu et al. 2005), iron-containing fly ash (Yi et al. 2009), iron-impregnated AC (Ghanizadeh et al. 2010; Vaughan and Reed 2005), zirconium-loaded AC (Daus et al. 2004; Peraniemi et al. 1994), silver and copper-impregnated AC (Rajakovic 1992), and zinc-preloaded magnetite nanoparticle (Yang et al. 2010) have been used for the removal of arsenic from the water/wastewater system. In order to enhance the process economy, the production of adsorbents from low-cost renewable biomass is usually encouraged as the surface modification of these adsorbents can further enhance the adsorptive removal of toxicants.

Pine cone (PC) is an agricultural waste which is derived in large quantity as an inexpensive biomass from the pine plantations made for pulp and paper industry (Ofomaja et al. 2009; Ayrilmis et al. 2009). The surface of PC contains various functional groups such as alcohols and aldehydes in its cellulose, hemicelluloses, and lignin fractions, which make it suitable for a series of chemical reactions (condensation, etherification, and copolymerization) and surface modifications (Benyoucef and Amrani 2011). Many studies have reported the utilization of PC as an effective biosorbent for the removal of Cu(II) and Pb(II) (Ofomaja et al. 2010), Cd(II) and Pb(II) (Argun et al. 2008), Cr(IV) (Ucun et al. 2008), phosphate ions (Benyoucef and Amrani 2011), textile dyes (Mahmoodi et al. 2011), phenol (Vazquez et al. 2006), and anionic surfactant sodium dodecyl sulfate (Sen et al. 2012).

Biochar is derived from thermal degradation of different organic materials (crop residue, forest by-product, and sewage sludge) and has been recommended as a multifunctional adsorbent for the removal of organic pollutants and heavy metals (Regmi et al. 2012). The difference in the adsorption behavior of biosorbent and biochar is mainly due to the differences in its physico-chemical properties like porosity, surface area, pore structure, chemical/elemental composition, and ash content (Varol and Putun 2012).

To the best of our knowledge, raw and chemically modified (Zn-loaded) PC biochar has not been exploited before for the removal of As(III) from the wastewater/drinking water. In this study, the adsorption potential of raw and modified PC biochar for the removal of As(III) from the aqueous solution was evaluated through a series of batch adsorption experiments. In order to gain an in-depth understanding of adsorption mechanism of As(III) onto raw and modified biochar, equilibrium isotherms, kinetics, and thermodynamic studies have been extensively carried out. Besides, the physico-chemical properties of the raw and modified PC biochars were examined using elemental analyzer, surface area analyzer, thermo-gravimetric analyzer, Fourier transform infrared spectroscopy, and scanning electron microscopy.

Materials and methods

Preparation of raw and Zn-loaded PC biochar

Pine cones were collected from the pine trees located in the campus of University of Ulsan, Korea. In order to remove the impurities, the collected pine cones were washed with deionized water and dried in an oven at 110 °C for 24 h. After drying, the material was crushed and sieved through a 1.18 mm standard mesh. The pyrolysis of fine PC powder (1.18 mm) was carried out in a fixed bed reactor having dimension of 45 cm × 10 cm (length × diameter). The powder samples were placed in the reactor at 500 °C temperature for 1 h with the purging of nitrogen at a flow rate of 0.1 m^3 h^{-1}. Finally, the pyrolized samples were washed three times with deionized water and dried in an oven at 90 °C overnight.

In order to prepare the metal-loaded PC biochar, 10 g of dried PC biochar was mixed with 100 mL of $Zn(NO_3)_2{\cdot}6H_2O$ precursor solution. The mixture was stirred at room temperature (25 °C) for 12 h. After filtration and washing, the Zn-loaded PC biochar was dried in an oven at 110 °C overnight. More details of impregnation method are available elsewhere (Rajakovic 1992; Ning et al. 2013).

Characterization of raw and Zn-loaded biochar

Elemental composition (C, H, N, S, and O) of biochar was determined by an elemental analyzer (Flash 2000, Thermo Scientific, Milan, Italy). Thermo-gravimetric (TG/DTA) analyzer (TA Q50 instrument, USA) was used for the determination of thermal properties of biochar, while the functional group analysis was conducted by a Fourier transform infrared spectrometer (Nicolet 380, Thermo Electron Co., USA) over 400–4,000 cm^{-1} using the KBr pellet technique. The surface physical morphology was examined using a field emission scanning electron

microscope (FE-SEM) (JSM-6500F, JEOL, Tokyo, Japan) operating at 10 kV. The surface porosity was measured by an ASAP 2020-Micromeritics apparatus, USA, and the specific surface area and pore volume were determined using Brunauer-Emmett-Teller (BET) method.

Batch adsorption experiments

Batch adsorption experiments were conducted using known amount of PC biochar with 50 mL of As(III) solution in 100-ml Erlenmeyer flasks. pH of the solution was adjusted by using 0.1 M standard solution of HCl/NaOH. The flasks were placed on a thermostat shaker stirred at 120 rpm and at ambient temperature (25 °C). After a specified time, suspension was filtered and analyzed for residual As(III) concentration by atomic absorption spectrophotometer (model AA240-2004, Varian, USA). Each experiment was conducted in duplicate under identical conditions and the average values were reported. The effect of pH on adsorption capacity was examined by varying the pH from 2 to 12 with the adsorbent and adsorbate doses of 10 g L^{-1} and 100 μg L^{-1}, respectively. In order to study the adsorption isotherm equilibrium, the experiments were conducted at initial concentrations of As(III) varying between 50 and 200 μg L^{-1}, at the adsorbent dose of 10 g L^{-1}. The kinetics of adsorption process was determined using the experimental data with adsorbent and adsorbate concentrations of 10 g L^{-1} and 100 μg L^{-1}, respectively. The samples were taken at regular interval of 1 h to determine the residual concentration of As(III) in the aqueous solution.

The amount of adsorption per gram of adsorbent, q (mg g^{-1}), was calculated by:

$$q = \frac{(C_0 - C)V}{W} \tag{1}$$

where C_0 and C are the concentrations of adsorbate in the solution at time zero and any time '*t*,' respectively, V is the working volume, and W is the mass of adsorbent dose.

Adsorption isotherms

The adsorption process is usually described through isotherms, i.e., the amount of adsorbate on the adsorbent (q_e) as a function of its concentration (C_e) at constant temperature. The Langmuir model equation is expressed as:

$$\frac{C_e}{q_e} = \frac{1}{bq_{max}} + \frac{C_e}{q_{max}} \tag{2}$$

where C_e is the concentration of As(III) in solution (mg L^{-1}) at equilibrium, q_e is the maximum As(III) uptake (mg g^{-1}), and b is the Langmuir equilibrium constant related to the free energy of adsorption and is the measure of adsorption affinity or heterogeneity. q_{max} is the maximum amount of As(III) per gram of adsorbent to form a complete monolayer on the surface. The Langmuir constants b and q_{max} are calculated from the slope and intercept of C_e/q_e versus C_e.

The Freundlich model is an empirical model and is described by the equation:

$$\log q_e = \log K_F + \frac{1}{n}\log C_e \tag{3}$$

where K_F is the measure of the adsorption capacity and n is a measure of the adsorption intensity.

Kinetic modeling

Three kinetic models, namely pseudo-first-order, pseudo-second-order, and intra-particle diffusion models were used to analyze and determine the suitable kinetic parameters. The pseudo-first-order kinetic model is described by:

$$\log(q_e - q_t) = \log q_e - \frac{k_1}{2.303}t \tag{4}$$

where k_1 (mg g^{-1} min) is pseudo-first-order adsorption rate constant that was obtained from the slopes of the linear plots of $\log(q_e - q_t)$ versus t, q_e and q_t are the amounts of adsorbate that adsorbed at equilibrium time, and time '*t*,' respectively.

The pseudo-second-order chemisorption kinetic model is given as:

$$\frac{t}{q_t} = \frac{1}{k_2 q_e^2} + \frac{1}{q_e}t \tag{5}$$

where k_2 (mg g^{-1} min). is pseudo-second-order adsorption rate constant and can be obtained from the plot of t/q_t against t.

In order to identify the diffusion mechanism in an adsorption process, intra-particle diffusion model was considered. It helps in understanding the rate controlling step affecting the kinetics and to figure out the degree of boundary layer control. It is represented by the following equation:

$$q_t = k_p t^{1/2} + c \tag{6}$$

where k_p and c are the intra-particle diffusion rate constant (mg g^{-1} $min^{1/2}$) and the intercept, respectively.

Thermodynamic studies

In order to calculate the thermodynamic parameters such as Gibb's free energy ($\Delta G°$), entropy ($\Delta S°$), and enthalpy ($\Delta H°$) changes in the adsorption process of As (III) with raw and Zn-loaded PC biochars, the following equation can be applied (Arias and Sen 2009; Karagöz et al. 2008).

Table 1 Properties of raw and Zn-loaded pine cone biochar

S. no.	Properties	Raw PC biochar	Zn-loaded PC biochar
1	Elemental composition (wt%)		
	C	67.88	71.21
	H	3.89	3.03
	O	22.07	20.43
	N	0.55	0.51
	S	<0.01	<0.01
	H/C	0.06	0.04
	O/C	0.33	0.29
2	Bulk density (kg m^{-3})[a]	216	256
3	Moisture (wt%)[b]	3.12	3.08
4	Ash (wt%)[b]	2.13	2.14
5	Volatile matter (wt%)[b]	27.22	18.99
6	Fixed carbon (wt%)[b]	67.53	75.79
7	pH^{c}_{PZC}	4.66	4.03
8	BET surface area (m^2 g^{-1})	6.60	11.54
9	Micropore volume (cm^3 g^{-1})	0.016	0.028

[a] Tamping procedure, Ofomaja et al. (2010)

[b] Modified thermal analysis, Ahmad et al. (2012)

[c] pH drift, Muniz et al. (2009)

$$\Delta G^{\circ} = \Delta H^{\circ} - T\Delta S^{\circ} \quad (7)$$

$$\log\left(\frac{q_e}{C_e}\right) = \frac{\Delta S^{\circ}}{2.303R} + \frac{-\Delta H^{\circ}}{2.303RT} \quad (8)$$

where q_e is the amount of arsenic adsorbed per unit mass of adsorbent (mg g^{-1}), C_e is the equilibrium concentration (mg L^{-1}), R is the gas constant (8.314 J mol^{-1} K^{-1}), and T is temperature in degree Kelvin.

Results and discussion

Physico-chemical characterization of PC biochar

As shown in Table 1, the elemental composition of PC biochar mainly consists of 67.88 and 22.07 wt% of carbon and oxygen, respectively. The molar ratios of these elements were used to estimate the aromaticity (H/C) and polarity (O/C) of biochar and were calculated as 0.06 and 0.33, respectively. PC biochar was highly carbonized at high temperature, and its low ash content (2.13 wt%) indicated the efficient thermal conversion process. The other physico-chemical characteristics of PC biochar are given in Table 1.

The surface properties of raw PC biochar were improved through the chemical modification, and a high BET surface area (11.543 m^2 g^{-1}) of Zn-loaded PC biochar was observed as compared to raw PC biochar (6.598 m^2 g^{-1}).

The thermal properties of raw and Zn-loaded biochars are illustrated in Fig. 1. Derivative thermo-gravimetric (DTG) curve of raw PC biochar revealed two exothermic peaks corresponding to two weight loss steps at 330 and 480 °C, respectively, whereas only one exothermic peak at 480 °C was observed in case of Zn-loaded PC biochar. The first weight loss step was associated with the decomposition of hemicellulose and cellulose fractions following lignin degradation in second weight loss step. The devolatilization of organic matters took place between 250 and 550 °C with a maximum weight loss at 480 °C, showing a sharp decrease in biochar weight. In case of Zn-

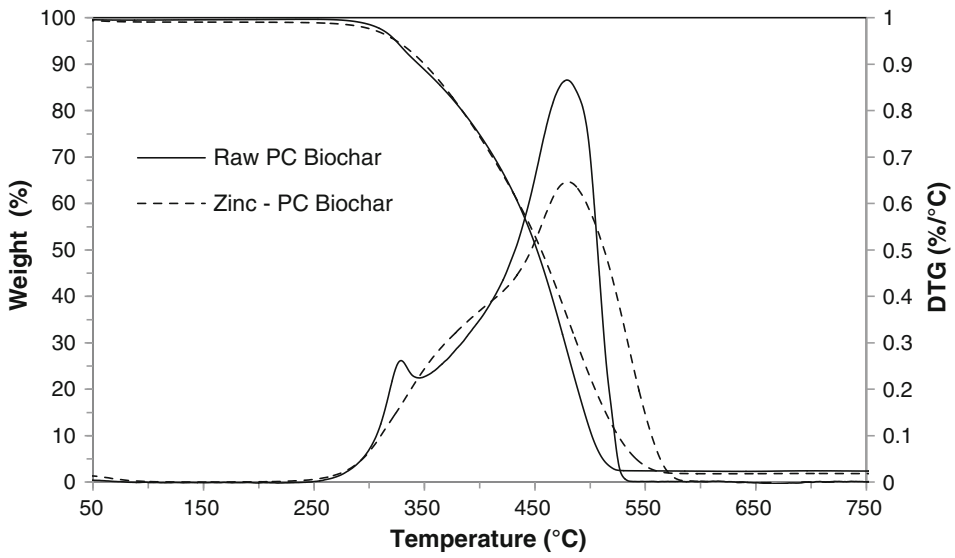

Fig. 1 The TG (**a**) and DTG (**b**) *curves* of raw and Zn-loaded pine cone biochar

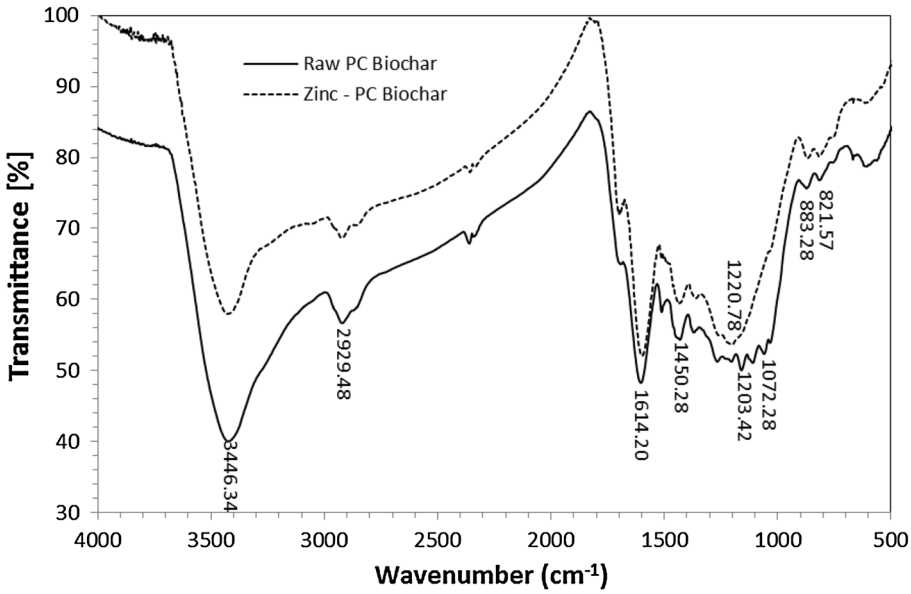

Fig. 2 The FTIR spectra of raw and Zn-loaded pine cone biochar

loaded PC biochar, the absence of first exothermic peak at 330 °C indicated the decomposition of cellulosic and hemicellulosic fractions during the surface modification process. Similar findings have been reported during the pyrolysis of rice husks and apricot stones (Sentorun-Shalaby et al. 2006; Williams and Besler 1993).

The FTIR spectra of raw and Zn-loaded biochar are illustrated in Fig. 2. Broad absorption bands in between 3,000 and 3,600 cm^{-1} were observed with a maximum peak at 3,434.34 cm^{-1} which can be assigned to the O–H stretching vibrations of hydrogen bonds. Spectra band observed at 2,929.4 cm^{-1} represents the aliphatic C–H group. Both raw and Zn-loaded PC biochar exhibit the peaks at around 1,614.20 cm^{-1} which can be ascribed to the C=O asymmetric stretching of ketones, aldehydes, lactones, or carboxyl groups (Momcilovic et al. 2011). The peaks in between 1,517.78–1,450.28 cm^{-1} represent the presence of aromatic rings or rings with C=C bonds. Besides, the peaks in between 1,203.42–1,072.28 cm^{-1} are attributed to the C–O stretching groups of carboxylic acid or due to the coupling of the stretching band of C–N, and the bending band of N–H (Li and Bai 2006; Martinez et al. 2006). Finally, the peaks in between 900 and 800 cm^{-1} were corresponding to the C–H_n aliphatic or aromatic bonds (Blazquez et al. 2012). The treatment of PC biochar with $Zn(NO_3)_2$ resulted in the disappearance of peak at 1,220.78 cm^{-1} and the appearance of multiple peaks in between 1,203.42 and 1,072.28 cm^{-1}. It can be demonstrated that the decomposition of hemicellulose and lignin components at high temperature leads to the breakage and rearrangement of stronger bonds in aromatic rings and carboxyl groups, with the evolution of additional N=O from $Zn(NO_3)_2$ modification (Srinivasan and Ganguly 1991).

Figure 3a, c shows the morphology and surface characteristics of raw and Zn-loaded PC biochar, respectively, before the adsorption. Similarly, Fig. 3b, d illustrates the surface texture and morphology of raw and Zn-loaded PC biochar, respectively, after the adsorption of As(III) from aqueous solution. The surface texture and morphology of both raw and modified biochars were different from one another. After the adsorption, the pores appearing on the surface have a fewer dimensions with smoother surface as compared to that before the adsorption. It is noteworthy that the chemical treatment of adsorbent has attributed the formation of porous structure that leads to an increase in internal surface as well as adsorption capacity (Zhang and Itoh 2005; Ofomaja et al. 2010).

Effect of pH on adsorption

Initial pH of the aqueous solution plays an important role in controlling the amount of As(III) adsorption onto the surface of biochar. Figure 4 represents the effect of varying pH on the removal efficiency of As(III) from the aqueous solution. Maximum adsorption capacity of As(III) was observed in the pH range of 2.0 and 4.0 for both raw and Zn-loaded PC biochars followed by a decrease with increase in the pH from 4.0 to 12.0. At pH 2.0, maximum As(III) adsorptive removal capacity of 5.3 and 7.0 μg g^{-1} onto raw and Zn-loaded PC biochars, respectively, were observed. Mohan et al. (2007) have reported maximum As(III) adsorption onto the biochar derived from oak bark, oak wood, pine bark, and pine wood in the pH range 2.0 to 4.0. The data from the Fig. 4 indicated that the Zn-loaded PC biochar was more efficient compared to the raw PC biochar for As(III) adsorption. The adsorption of As(III) on

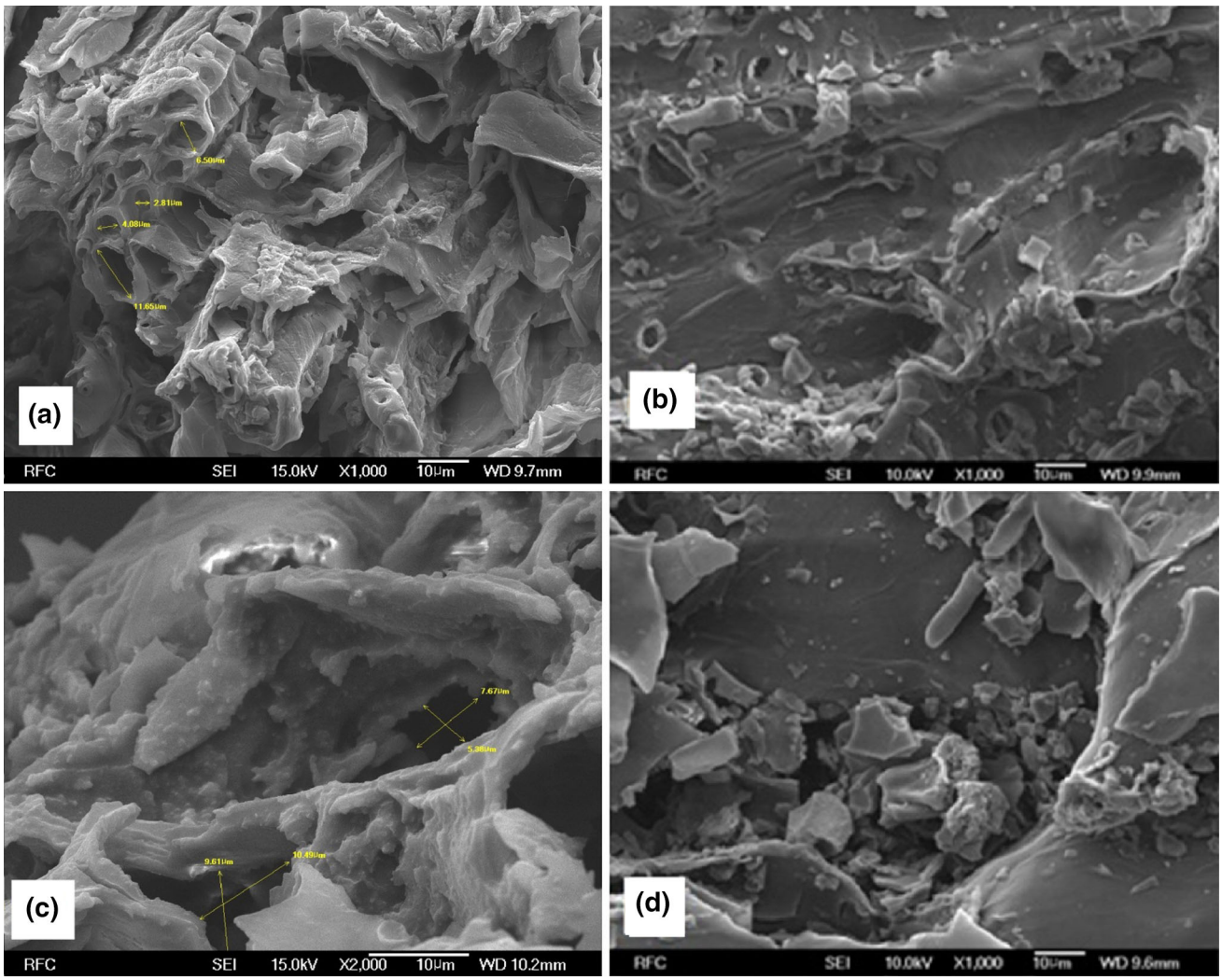

Fig. 3 The SEM micrographs of raw PC biochar samples before and after adsorption of arsenic(III) (**a**, **b**), and Zn-loaded PC biochar samples before and after adsorption of arsenic (III) (**c**, **d**), respectively

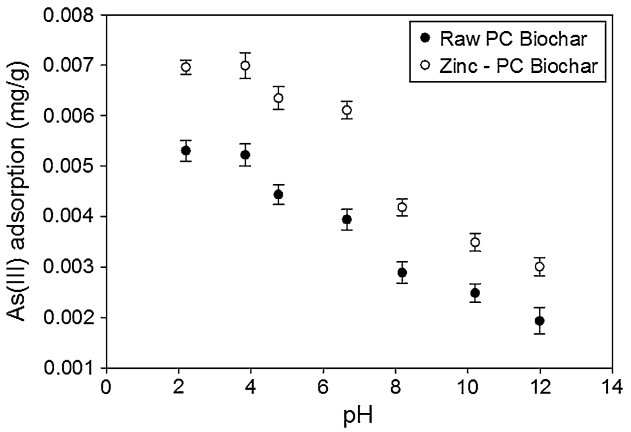

Fig. 4 The effect of pH on As(III) removal onto raw and Zn-loaded PC biochar

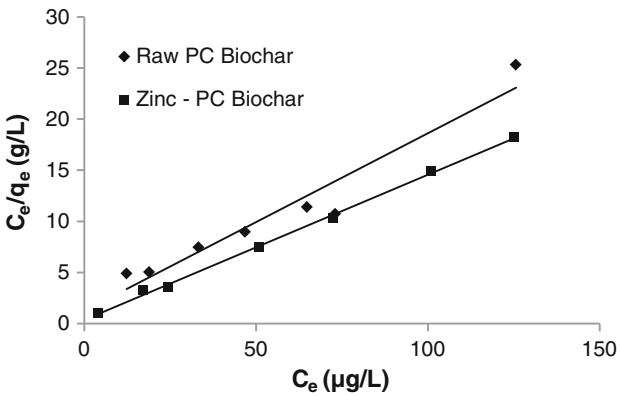

Fig. 5 Langmuir plot for the adsorption of arsenic by raw and Zn-loaded pine cone biochar

PC biochar with or without metal was dependent on the arsenic valence and the pH of the solution. In the aqueous solution, As(III) exists either as neutral or slightly charged species which is not readily oxidized at basic pH values. Hence, its uptake at high pH would be obviously low (Pattanayak et al. 2000). Physical adsorption was mainly responsible for the As(III) adsorption onto raw PC biochar, while chemisorption played additional role for As(III) adsorption onto Zn-loaded PC biochar (Rajakovic 1992) (Fig. 5).

It has been reported that H_3AsO_3 and $H_2AsO_3^-$ are the predominant As(III) species available in the aqueous solution in the pH range of 4 to 9.5 (Rajakovic 1992; Ayoob et al. 2007; Mondal et al. 2007). Both the surfaces of raw and Zn-loaded PC biochars were positively charged up to their pH_{PZC} value of 4.66 and 4.03, respectively, and the adsorption primarily occurred through the electrostatic attractions between the neutral/negative arsenic species and positively charged biochar surface. Furthermore, with the increase in pH up to 7.0, a decrease in adsorption of As(III) was observed which was mainly due to the Van der Waals interaction between the neutral arsenic species and biochar surface. Above the pH 7.0, a sharp decrease in adsorption was observed due to the increase in electrostatic repulsion between the negative surface sites of adsorbent and the dominating negative arsenic species of $H_2AsO_3^-$ and $HAsO_3^{2-}$.

Therefore, the overall effect of pH on the pattern of arsenic removal onto both raw and Zn-loaded biochars within the pH range of 2–12 was quite similar, though to different extent. The impregnation of Zn onto biochar surface resulted in the increase in positive charge intensity at acidic pH of 2–4 that favored the higher As(III) removal efficiency. The removal of arsenic is highly dependent on solution pH and is influenced by the surface charge of adsorbent, degree of ionization, and the nature of arsenic species in solution (Hlavay and Polyak 2005; Ayoob et al. 2007).

The following reaction mechanism might be involved in the As(III) adsorption onto Zn-loaded biochar (Payne and Abdel-Fattah 2005).

$$Z(A)\text{-}[Zn\text{-}OH]^+ + (ads)H\text{-}OAs(OH)_2$$

For As(III) adsorption at pH < 7

$$Z(A)\text{-}Zn\text{-}O\text{-}H^+ + (ads)\text{-}O\text{-}As(OH)_2$$

For As(III) adsorption at pH > 7

In the aqueous solution, As(III) exists in various anionic forms, viz. AsO_3^{3-}, $HAsO_3^{2-}$, and H_2AsO^{3-} especially at pH > 9.0, while it appear in a little dissociated form in the pH range of 6.0 to 9.0. The chemisorption of As(III) might occur through the formation of surface complexes between the soluble arsenic species and the surface hydroxyl groups

Table 2 Equilibrium isotherm and kinetic model parameters for removal of As(III) with raw and Zn-loaded PC biochar

Adsorbent	Equilibrium isotherms								
	Langmuir isotherm				Freundlich isotherm				
	q_{max} (mg g^{-1})		b	R^2	K_F		n	R^2	
Raw biochar	0.0057		140.459	0.9339	1.302		2.97	0.7086	
Zn-loaded biochar	0.007		396.427	0.9979	3.657		6.84	0.7962	
Adsorbent	Kinetic models								
	Pseudo-first order				Pseudo-second order			The intra-particle diffusion	
	$q_{e,cal}$ (mg g^{-1})	k_1 (mg g^{-1} min^{-1})	R^2		$q_{e,cal}$ (mg g^{-1})	k_2 (mg g^{-1} min^{-1})	R^2	k_p (mg g^{-1} min$^{-1/2}$)	c (mg g^{-1})	R^2
Raw biochar	0.004	0.006	0.9409		0.0061	0.040	0.9746	0.0003	0.0008	0.9587
Zn-loaded biochar	0.0057	0.0094	0.9561		0.0083	0.282	0.9941	0.0004	0.0019	0.9981

created by zinc modification (Payne and Abdel-Fattah 2005).

Adsorption isotherms

The performances of raw and Zn-loaded PC biochar were systematically evaluated using the Langmuir and Freundlich isotherm models by examining the distribution pattern of As(III) between the liquid phase and solid surface of PC biochar during the As(III) surface adsorption/chemisorption process. Table 2 shows that the experimental data of raw and Zn-loaded PC biochars were well fitted to the Langmuir isotherm with high R^2 (0.93 and 0.99, respectively) as compared to the Freundlich model ($R^2 = 0.70$ and 0.76, respectively). The Langmuir isotherm represents the monolayer coverage of As(III) onto the surface of raw and Zn-loaded PC biochar. This isotherm assumes that the adsorption free energy is independent of both the surface coverage and the monolayer formation. The Langmuir monolayer coverage is defined by adsorption capacity (q_{max}), which was found to be 5.7 μg g^{-1} for As(III) adsorption on raw biochar and 7.0 μg g^{-1} on Zn-loaded biochar with the initial adsorbate concentration of 100 μg L^{-1}. In Langmuir isotherm model, b represents the binding energy of the adsorption system and the degree of sorption affinity of adsorbate [As(III)] toward the PC

Table 3 Comparative evaluation of various low-cost adsorbents for arsenic(III) removal

Adsorbents	Type of water	pH	Arsenic concentration	Surface area (m^2 g^{-1})	Model	Adsorption capacity (mg g^{-1})	References
Pine wood char	Drinking water	3.5	10–100 μg L^{-1}	2.73	Langmuir	0.0012	Mohan et al. (2007)
Char-carbon derived from fly ash	Aqueous solution	3.1	193–992 mg L^{-1}	36.48	NS	89.2	Pattanayak et al. (2000)
Activated carbon	Aqueous solution	5.4	193–992 mg L^{-1}	43.4	NS	29.9	Pattanayak et al. (2000)
ZME (Oaxaca)[a]	Ground water	4.0	0.1–4 mg L^{-1}	51	Langmuir	0.0028	González et al. (2001)
ZMS (San Luis Potosi)[a]	Ground water	4.0	0.1–4 mg L^{-1}	22	Langmuir	0.017	González et al. (2001)
Mn-minerals and Fe-oxides	Drinking water	3.0	0.1–100 mg L^{-1}	40.8	NS	14.7	Deschamps et al. (2005)
Biomass	Aqueous solution	5.0	200 mg L^{-1}	NS	NS	NS	Teixeira and Ciminelli (2005)
Fe modified AC	Ground water	7.0–11	50 μg L^{-1}	1,200	Langmuir	NS	Payne and Abdel-Fattah (2005)
Fe modified Clinoptilolite	Ground water	7.0–10	50 μg L^{-1}	40	NS	NS	Payne and Abdel-Fattah (2005)
Fresh biomass	Ground water	6.0–8.0	100 mg L^{-1}	NS	NS	128.1	Kamala et al. (2005)
Modified calcined bauxite	Ground water	~7.0	1–2 mg L^{-1}	NS	Freundlich	1.362	Ayoob et al. (2007)
Activated Carbon[b]	Drinking water	7.9	5–20 mg L^{-1}	1,030	Langmuir	1.393	Budinova et al. (2006)
Iron oxide-coated sand	Drinking water	7.6	100 μg L^{-1}	10.6	Langmuir	0.041	Thirunavukkarasu et al. (2003)
Iron oxide-coated sand	Ground water	7.5	100 μg L^{-1}	NS	Langmuir	0.0285	Gupta et al. (2005)
Uncoated sand	Ground water	7.5	100 μg L^{-1}	NS	Langmuir	0.0056	Gupta et al. (2005)
Raw PC biochar	Aqueous solution	4	100 μg L^{-1}	6.59	Langmuir	0.0057	This study
Zinc-loaded PC biochar	Aqueous solution	4	100 μg L^{-1}	11.54	Langmuir	0.0070	This study

NS not specified, *AC* activated carbon, *PC* pine cone

[a] Derived from natural zeolites, volcanic stone, and cactaceous powder

[b] Carbon A, from Olive Pulp and Olive Stones

biochar. A high affinity of Zn-loaded biochar ($b = 396.43$) toward As(III) species was observed when compared to the affinity of raw PC biochar ($b = 140.46$).

The essential characteristic of Langmuir isotherm is represented by a dimensionless separation factor (R_L) which represents the ratio of the unused adsorbent capacity to the maximum adsorbent capacity (Ayoob et al. 2007). This is given by the Eq. (9):

$$R_L = \frac{1}{1 + bC_0} \tag{9}$$

where C_0 is the initial As(III) concentration (mg L^{-1}) and b is the Langmuir isotherm constant. In this study, the value of R_L is calculated as 0.065 and 0.024 for As(III) adsorption onto raw and Zn-loaded PC biochar, respectively, indicating favorable adsorption of As(III) onto both raw and Zn-loaded PC biochar at ambient temperature (25 °C).

The maximum As(III) adsorption capacity of raw and Zn-loaded PC biochar as obtained from the Langmuir model were 5.7 and 7.0 μg g^{-1}, respectively, which is comparable to the findings of other researchers (Table 3). Almost similar uptake have been reported at equilibrium following the Langmuir model for Zeolite (ZME) (González et al. 2001), iron oxide-coated/iron oxide-uncoated sand (Gupta et al. 2005), and pine wood char (Mohan et al. 2007) (Table 3).

Kinetic modeling

Table 2 also represents the kinetic parameters evaluated by fitting the experimental data to pseudo-first-order, pseudo-second-order, and intra-particle diffusion models. It was observed that the pseudo-second-order model well fitted to the experimental data derived from raw and Zn-loaded PC biochar with R^2 of 0.95 and 0.99, respectively. A comparatively high As(III) uptake rate (k_2) of 0.282 mg g^{-1} min was observed on Zn-loaded PC biochar when compared to the uptake rate of 0.040 mg g^{-1} min on raw PC biochar. Moreover, in both cases, $q_{e,cal}$ values of

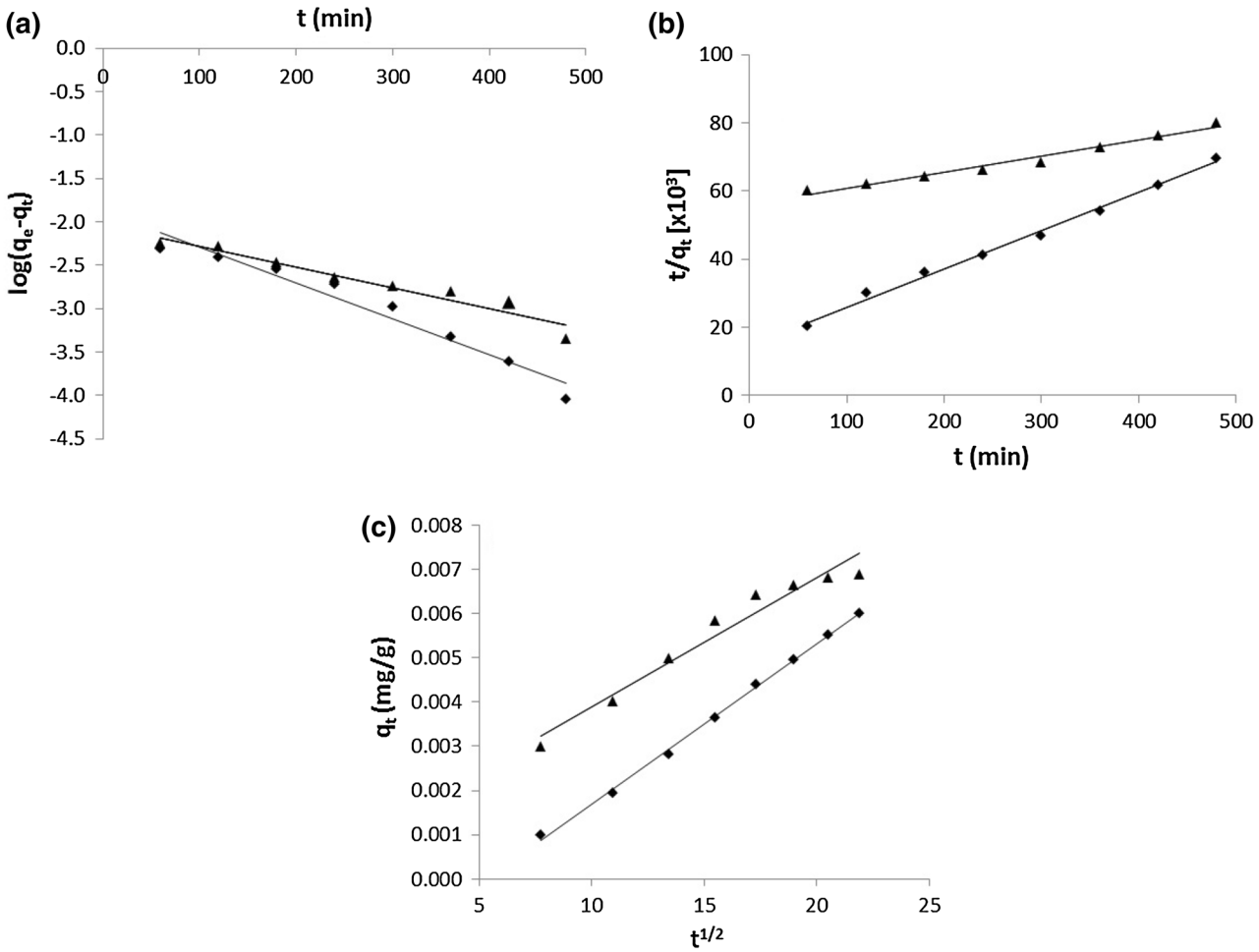

Fig. 6 Kinetic models for adsorption of As(III) onto raw (▲) and Zn-loaded (◆) PC biochar; **a** Pseudo-first-order, **b** Pseudo-second-order, and **c** the intra-particle diffusion

Table 4 Thermodynamic parameters for removal of arsenic(III) at different temperatures

Adsorbent	Temperature (K)	$\Delta H°$ (kJ mol^{-1})	$\Delta S°$ (kJ mol^{-1} K^{-1})	$\Delta G°$ (kJ mol^{-1})
Raw PC biochar	293			−3.74
	303	13.25	0.058	−4.32
	318			−5.19
Zinc-loaded PC biochar	293			−10.21
	303	31.10	0.141	−11.62
	318			−13.74

0.0061 and 0.0083 mg g^{-1} were very close to the experimental $q_{e,exp}$ values (Fig. 6a, b).

The intra-particle diffusion plot shows some degree of nonlinearity between As(III) uptake (μg/g) and $t^{1/2}$ for adsorption on raw PC biochar (Fig. 6c). Here, As(III) uptake (q_t) occurred in two steps: a sharper exponential linear portion attributed to the diffusion of As(III) species to the external surface of raw PC biochar through boundary layer diffusion followed by the intra-particle diffusion as indicated by a second gradual linear portion (Fig. 6c) (Tsibranska and Hristova 2011). The rate of uptake of As(III) might be affected by the size of adsorbate molecules, its concentration and affinity toward adsorbent, distribution coefficients of As(III) in bulk, and the pore size distribution of adsorbent. The adsorption of As(III) on Zn-loaded PC biochar was mainly controlled by boundary layer diffusion as represented by a sharp linear plot, but some degree of intra-particle diffusion was also responsible as the plot do not pass through origin ($c = 0.0019$).

Thermodynamic studies

The entropy ($\Delta S°$) and enthalpy ($\Delta H°$) values of adsorption were obtained from a linear plot of $log(q_e/C_e)$ versus $1/T$ using Eq. (8) under three temperature ranges at 293 K, 303 K, and 313 K (Table 4). The calculated free energy ($\Delta G°$) was negative which indicated the feasibility of the process and spontaneous nature of the adsorption process in both the cases of raw and Zn-loaded biochar. The positive $\Delta H°$ values (13.25 and 31.10 kJ mol^{-1}) in case of raw and Zn-loaded biochar, respectively, indicated the exothermic nature of adsorption interaction. The positive values of $\Delta S°$ (0.058 and 0.141 kJ mol^{-1} K^{-1}) showed an increase in randomness at the solid/solution interface during the adsorption of As(III) on raw and Zn-loaded PC biochar, respectively.

Conclusion

This study examined the practicality of PC biochar (raw and Zn-loaded) to use as promising adsorbents for the removal of As(III) from aqueous solution. Adsorptive removal of As(III) on raw and Zn-loaded PC biochar were found to be consistent over an acidic pH range of 2–4, which decreased further with an increase in solution pH. The adsorption capacity of As(III) was enhanced from 5.7 to 7.0 μg g^{-1} through surface modification of PC biochar by $Zn(NO_3)_2$ impregnation. Langmuir model was well fitted to the equilibrium data which revealed highly favorable monolayer As(III) adsorption onto raw/Zn-loaded PC biochar. Kinetic study indicated the pseudo-second-order As(III) adsorption that was controlled by boundary layer diffusion with some extent of intra-particle diffusion. Besides, the exothermic and spontaneous nature of As(III) adsorption onto raw and Zn-loaded biochar justifies its effectiveness as a low-cost adsorbent for As(III) removal from surface/ground water.

Acknowledgments This work was supported by the research funds from the University of Ulsan in South Korea during the financial year 2012–2013.

References

Ahmad M, Lee SS, Dou X, Mohan D, Sung JK, Yang JE, Ok YS (2012) Effects of pyrolysis temperature on soybean stover- and peanut shell-derived biochar properties and TCE adsorption in water. Bioresour Technol 118:536–544

Akter A, Ali MH (2011) Arsenic contamination in groundwater and its proposed remedial measures. Int J Environ Sci Technol 8:433–443

Argun ME, Dursun S, Karatas M, Guru M (2008) Activation of pine cone using Fenton oxidation for Cd(II) and Pb(II) removal. Bioresour Technol 99:8691–8698

Arias F, Sen TK (2009) Removal of zinc metal ion (Zn^{2+}) from its aqueous solution by kaolin clay mineral: a kinetic and equilibrium study. Colloids Surf A Physicochem Eng Asp 348:100–108

Ayoob S, Gupta AK, Bhakat PB (2007) Performance evaluation of modified calcined bauxite in the sorptive removal of arsenic(III) from aqueous environment. Colloids Surf A Physicochem Eng Asp 293:247–254

Ayrilmis N, Buyuksari U, Avci E, Koc E (2009) Utilization of pine (*Pinus pinea* L.) cone in manufacture of wood based composite. For Ecol Manag 259:65–70

Benyoucef S, Amrani M (2011) Adsorption of phosphate ions onto low cost Aleppo pine adsorbent. Desalination 275:231–236

Blazquez G, Martin-Lara MA, Dionisio-Ruiz E, Tenorio G, Calero M (2012) Copper biosorption by pine cone shell and thermal decomposition study of the exhausted biosorbent. J Ind Eng Chem 18:1741–1750

Budinova T, Petrov N, Razvigorova M, Parra J, Galiatsatou P (2006) Removal of arsenic(III) from aqueous solution by activated carbons prepared from solvent extracted olive pulp and olive stones. Ind Eng Chem Res 45:1896–1901

Daus B, Wennrich R, Weiss H (2004) Sorption materials for arsenic removal from water: a comparative study. Water Res 38:2948–2954

Deschamps E, Ciminelli VST, Holl WH (2005) Removal of As(III) and As(V) from water using a natural Fe and Mn enriched sample. Water Res 39:5212–5220

Ghanizadeh G, Ehrampoush MH, Ghaneian MT (2010) Application of iron impregnated activated carbon for removal of arsenic from water. Iran J Environ Health Sci Eng 7:145–156

González MPE, Mattusch J, Einicke WD, Wennrich R (2001) Sorption on natural solids for arsenic removal. Chem Eng J 81:187–195

Gu Z, Fang J, Deng B (2005) Preparation and evaluation of GAC-based Iron-containing adsorbents for arsenic removal. Environ Sci Technol 39:3833–3843

Guo H, Stüben D, Berner Z (2007) Arsenic removal from water using natural iron mineral-quartz sand columns. Sci Total Environ 377:142–151

Gupta VK, Mittal A, Krishnan L (2005) Adsorption of As(III) from aqueous solutions by iron oxide-coated sand. J Colloid Interface Sci 288:55–60

Hlavay J, Polyak K (2005) Determination of surface properties of iron hydroxide-coated alumina adsorbent prepared for removal of arsenic from drinking water. J Colloid Interface Sci 284:71–77

Kamala CT, Chu KH, Chary NS, Pandey PK, Ramesh SL, Sastry ARK, Sekhar KC (2005) Removal of arsenic(III) from aqueous solutions using fresh and immobilized plant biomass. Water Res 39:2815–2826

Kamsonlian S, Suresh S, Ramanaiah V, Majumder CB, Chand S, Kumar A (2012) Biosorptive behaviour of mango leaf powder and rice husk for arsenic(III) from aqueous solutions. Int J Environ Sci Technol 9:565–578

Karagöz S, Tay T, Ucar S, Erdem M (2008) Activated carbons from waste biomass by sulfuric acid activation and their use on methylene blue adsorption. Bioresour Technol 99:6214–6222

Li N, Bai R (2006) Highly enhanced adsorption of lead ions on chitosan granules functionalized with Poly(acrylic acid). Ind Eng Chem Res 45:7897–7904

Mafu LD, Msagati TAM, Mamba BB (2013) Adsorption studies for the simultaneous removal of arsenic and selenium using naturally prepared adsorbent materials. Int J Environ Sci Technol. doi:10.1007/s13762-013-0374-1

Mahmoodi NM, Hayati B, Arami M, Lan C (2011) Adsorption of textile dyes on pine cone from colored wastewater: kinetic, equilibrium and thermodynamic studies. Desalination 268:117–125

Mandal BK, Suzuki KT (2002) Arsenic round the world: a review. Talanta 58:201–235

Manju GN, Raji C, Anirudhan TS (1998) Evaluation of coconut husk carbon for the removal of arsenic from water. Water Res 32:3062–3070

Martinez M, Miralles N, Hidalgo S, Fiol N, Villaescusa I, Poch J (2006) Removal of lead(II) and cadmium(II) from aqueous solutions using grape stalk waste. J Hazard Mater 133:203–211

Mohan D, Pittman CUJ (2007) Arsenic removal from water/wastewater using adsorbents—a critical review. J Hazard Mater 142:1–53

Mohan D, Pittman CUJ, Bricka M, Smith F, Yancey B, Mohammad J, Steele PH, Franco MFA, Serrano VG, Gong H (2007) Sorption of arsenic, cadmium, and lead by chars produced from fast pyrolysis of wood and bark during bio-oil production. J Colloid Interface Sci 310:57–73

Momcilovic M, Purenovic M, Bojic A, Zarubica A, Randelovic M (2011) Removal of lead(II) ions from aqueous solutions by adsorption onto pine cone activated carbon. Desalination 276:53–59

Mondal P, Balomajumder C, Mohanty B (2007) A laboratory study for the treatment of arsenic, iron, and manganese bearing ground water using Fe^{3+} impregnated activated carbon: effects of shaking time, pH and temperature. J Hazard Mater 144: 420–426

Muniz G, Fierro V, Celzard A, Furdin G, Sanchez GG, Ballinas ML (2009) Synthesis, characterization and performance in arsenic removal of iron-doped activated carbons prepared by modification with Fe(III) and Fe(II). J Hazard Mater 165:893–902

Ning P, Qiu J, Wang X, Liu W, Chen W (2013) Metal loaded zeolite adsorbent for hydrogen cyanide removal. J Environ Sci 25(4):808–814

Ofomaja AE, Naidoo EB, Modise SJ (2009) Removal of copper(II) from aqueous solution by pine and base modified pine cone powder as biosorbent. J Hazard Mater 168:909–917

Ofomaja AE, Naidoo EB, Modise SJ (2010) Biosorption of copper(II) and lead(II) onto potassium hydroxide treated pine cone powder. J Environ Manag 91:1674–1685

Pattanayak J, Mondal K, Mathew S, Lalvani SB (2000) A parametric evaluation of the removal of As(V) and As(III) by carbon-based adsorbents. Carbon 38:589–596

Payne KB, Abdel-Fattah TM (2005) Adsorption of arsenate and arsenite by Iron-treated activated carbon and zeolites: effects of pH, temperature, and ionic strength. J Environ Sci Health 40:723–749

Peraniemi S, Hannonen S, Mustalahti H, Ahlgren M (1994) Zirconium-loaded activated charcoal as an adsorbent for arsenic, selenium and mercury. Fresenius J Anal Chem 349:510–515

Rajakovic LV (1992) The sorption of arsenic onto activated carbon impregnated with metallic silver and copper. Separ Sci Technol 27:1423–1433

Regmi P, Moscoso JLG, Kumar S, Cao X, Mao J, Schafran G (2012) Removal of copper and cadmium from aqueous solution using switchgrass biochar produced via hydrothermal carbonization process. J Environ Manag 109:61–69

Sen TK, Thi TT, Afroze S, Phan C, Ang M (2012) Removal of anionic surfactant sodium dodecyl sulphate from aqueous solution by adsorption onto pine cone biomass of *Pinus radiate*: equilibrium, thermodynamic, kinetics, mechanism and process design. Desalin Water Treat 45:263–275

Sentorun-Shalaby C, Ucak-Astarlioglu MG, Artok L, Sarici C (2006) Preparation and characterization of activated carbons by one-step steam pyrolysis/activation from apricot stones. Micro Meso Mater 88:126–134

Srinivasan SK, Ganguly S (1991) FT-IR spectroscopic studies of metal nitrates supported on a modified montmorillonite clay. Catal Lett 10:279–288

Teixeira MC, Ciminelli VST (2005) Development of a biosorbent for arsenite: structural modeling based on X-ray spectroscopy. Environ Sci Technol 39:895–900

Thirunavukkarasu OS, Viraraghavan T, Subramanian KS (2003) Arsenic removal from drinking water using iron oxide-coated sand. Water Air Soil Pollut 142:95–111

Tsibranska I, Hristova E (2011) Comparison of different kinetic models for adsorption of heavy metals onto activated carbon from apricot stones. Bulg Chem Commun 43(3):370–377

Ucun H, Bayhan YK, Kaya Y (2008) Kinetic and thermodynamic studies of the biosorption of Cr(VI) by *Pinus sylvestris* Linn. J Hazard Mater 153:52–59

Urík M, Littera P, Ševc J, Kolenčík M, Čerňanský S (2009) Removal of arsenic (V) from aqueous solutions using chemically modified sawdust of spruce (*Picea abies*): kinetics and isotherm studies. Int J Environ Sci Techol 6:451–456

Varol EA, Putun AE (2012) Preparation and characterization of pyrolytic chars from different biomass samples. J Anal Appl Pyrol 98:29–36

Vaughan RLJ, Reed BE (2005) Modeling As(V) removal by a iron oxide impregnated activated carbon using the surface complexation approach. Water Res 39:1005–1014

Vazquez G, Alonso R, Freire S, Gonzalez-Alvarez J, Antorrena G (2006) Uptake of phenol from aqueous solutions by adsorption in a *Pinus pinaster* bark bed. J Hazard Mater B133:61–67

Williams PT, Besler S (1993) The pyrolysis of rice husks in a thermogravimetric analyser and static batch reactor. Fuel 72:151–159

Yang W, Kan AT, Chen W, Tomson MB (2010) pH-dependent effect of zinc on arsenic adsorption to magnetite nanoparticles. Water Res 44:5693–5701

Yi L, Fu-Shen Z, Fu-Rong X (2009) Arsenic(V) removal from aqueous system using adsorbent developed from a high iron-containing fly ash. Sci Total Environ 407:5780–5786

Zhang F-S, Itoh H (2005) Iron oxide–loaded slag for arsenic removal from aqueous system. Chemosphere 60:319–325